Journal of Engineering Technology and Applied Physics

Mantis Search Algorithm Based SHEPWM for Five-Phase Multilevel Inverter

Quan Ming Wong[1], Wei Tik Chew[1], Siok Lan Ong[2], Yee Wei Sea[1], Noor Syafawati Ahmad[1], Ahmad Firdaus Ahmad Zaidi[1] and Jenn Hwai Leong[1, *]

[1]*Faculty of Electrical Engineering Technology, Universiti Malaysia Perlis, 02600 Arau, Perlis, Malaysia.*

[2]*Faculty of Electronic Engineering Technology, Universiti Malaysia Perlis, 02600 Arau, Perlis, Malaysia.*

**Corresponding author*: jhleong@unimap.edu.my, *ORCiD*: 0009-0003-6135-7644

https://doi.org/10.33093/jetap.2026.8.1.5

Manuscript Received: 30 June 2025, Revised: 31 August 2025, Accepted: 9 October 2025, Published: 15 March 2026

***Abstract*—Large electric vehicles are being introduced as replacements for conventional heavy internal combustion engine (ICE) vehicles, aiming to mitigate environmental concerns. Five-phase electric motors are suggested as propulsion units in these vehicles due to their advantages in torque smoothness and fault tolerance. Driving electric motors requires converting DC power into AC using power converters. Among the available options, multilevel inverters (MLIs) are one option that suits this power conversion process. Compared to a conventional two-level inverter, the MLI offers the advantages of producing low-distortion output AC voltage with lower voltage stress on power switches and higher overall efficiency. However, determining the switching angles for the MLI is challenging. In this work, mantis search algorithm (MSA)-based selective harmonic elimination pulse width modulation (SHEPWM) technique is proposed to compute the switching angles for a five-phase MLI. The MSA-SHEPWM method is compared to that of genetic algorithm (GA) and particle swarm optimization (PSO) in terms of the objective function. The switching angles obtained using MSA-SHEPWM are capable of producing a low-distorted AC output voltage, in which the desired fundamental voltage is sustained while undesired low-order harmonics are successfully minimized. The effectiveness of the proposed algorithm has been validated through MATLAB and PSIM simulations.**

Keywords*—Multilevel Inverter, Pulse Width Modulation, Selective Harmonic Elimination, Switching-angle computation, Mantis Search Algorithm.

I. INTRODUCTION

Internal combustion engine (ICE) vehicles are among the primary sources of carbon dioxide emissions. To address this, replacing traditional ICEs with battery-powered electric vehicles (EVs) is strongly encouraged [1-2]. In this transition, five-phase electric motors are gaining attention as propulsion units due to their superior advantages in torque smoothness and fault tolerance compared to three-phase electric motors [3]. Since most of the battery provides direct current (DC) while the electric motors in the EVs conventionally require alternating current (AC), an inverter is necessary. Among various inverters, multilevel inverters (MLIs) are highly considered for the DC-AC conversion process to drive multiphase motors due to their capability in generating low-distortion AC output voltage with lower voltage stress on power switches and higher efficiency compared to traditional 2-level pulse-width modulation (PWM) inverters [4]. The main types of MLI topologies include neutral-point-clamped MLI (NPCMLI), flying capacitor MLI (FCMLI) and cascaded H-bridge MLI (CHBMLI) [5-6]. Among these topologies, CHBMLI offers higher modularity, reliability and simplicity in control [7-8].

Determining appropriate switching angles for MLIs to produce a low-distortion AC output voltage is challenging. Several conventional PWM techniques, such as sinusoidal PWM and space vector PWM techniques, have been proposed [9-11]. However, these techniques control the active solid-state switches in the MLI to operate at high switching frequency, leading to high switching losses. These switching losses can be reduced by applying the selective harmonic elimination PWM (SHEPWM) technique to the MLIs [12-13]. This technique determines the switching angles used to control the active solid-state switches in the MLI to operate at fundamental frequency to produce a sinusoidal-like staircase AC output waveform. The determined switching angles using the technique can control the fundamental voltage while eliminating or minimizing undesired low-order harmonics. However, determining the switching angles conventionally requires solving multiple non-linear harmonic equations

Published by MMU PRESS. URL: https://journals.mmupress.com/index.php/jetap/index

simultaneously, which presents a significant computational challenge. In [14-15], the equations can be solved using the Newton-Raphson (NR) method. However, this method is highly dependent on the guesses of initial switching angles, which are crucial for ensuring convergence. Selecting appropriate initial switching angles can be time-consuming, as poor initial guesses may lead to divergence or failure to find a valid solution. To overcome this issue, the harmonic equations are transformed into polynomial equations, which are then solved using resultant theory [16-17]. However, solving the polynomial equations is generally more complex, especially at a higher number of voltage levels, than solving the harmonic equations directly with the NR method. In [18], the harmonic equations are converted into an objective function, which is then solved using soft-computing (SC) method. This method is less dependent on the initial switching-angle guesses compared to the NR method and is simpler to implement than the resultant theory-based method. However, SC methods cannot provide switching angles that can exactly solve the harmonic equations; instead, they only provide approximate switching angles that are close to the exact solution. Hence, identifying the switching angles that closely match the exact solution using SC methods remains a challenging task. Among the various SC methods, genetic algorithm (GA) and particle swarm optimization (PSO) are employed to determine the switching angles [19-21]. However, both GA and PSO are prone to getting trapped in local minima when solving the SHEPWM problem in MLIs. This may occur due to the insufficient capabilities of their algorithms in exploration and exploitation, which limit their ability to find better solutions. To address this limitation, it is desirable to explore an alternative SC method with the potential to outperform GA and PSO in determining better switching angles.

In [22], an SC method, the mantis search algorithm (MSA) was introduced. This SC method has successfully addressed various optimization problems, including the characterization of silver nanoparticles, characterization of PV Panel, economic dispatch in combined heat and power systems, parameter optimization for multimodal biometric recognition and pattern recognition of partial discharge faults in switchgear [23-27]. However, MSA has not yet been applied to solve the SHEPWM problem in five-phase MLI. Therefore, in this paper, the MSA is proposed to solve the SHEPWM problem for a five-phase seven-level CHBMLI. To evaluate its performance, MSA is compared with GA and PSO in terms of objective function using MATLAB simulations. For further validation, the switching angles obtained from MSA are implemented in a five-phase seven-level CHBMLI model in PSIM software.

II. FIVE-PHASE SEVEN-LEVEL CHBMLI

A. Topology

Figure 1 illustrates the circuit topology of a five-phase seven-level CHBMLI. The figure shows that each phase of the seven-level CHBMLI consists of three identical H-bridge (HB) modules connected in series, denoted as HB1, HB2 and HB3. Each HB module is a full bridge circuit, comprising a DC voltage source (V_{dc}) and four active solid-state switches (SW_1, SW_2, SW_3 and SW_4). It is assumed that all V_{dc} have equal magnitudes. Every HB module can produce an output voltage waveform with three DC voltage levels of $+1V_{dc}$, $0V_{dc}$ and $-1V_{dc}$. By applying a proper switching state and three switching angles (α_1, α_2 and α_3), the summation of the output voltages generated by the three HB modules in each phase can synthesize a staircase seven-level output phase voltage (V_{ph}) waveform, involving $+3V_{dc}$, $+2V_{dc}$, $+1V_{dc}$, $0V_{dc}$, $-1V_{dc}$, $-2V_{dc}$ and $-3V_{dc}$, as shown in Fig. 2.

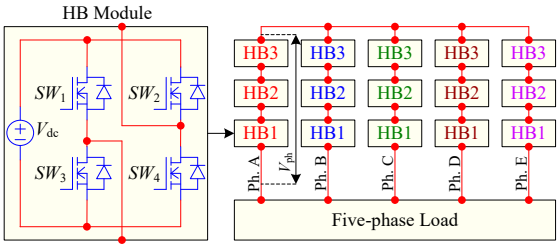

Fig. 1. Five-phase seven-level CHBMLI.

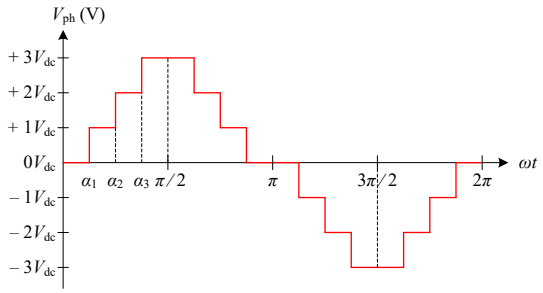

Fig. 2. Output V_{ph} of five-phase seven-level CHBMLI.

B. Switching State

Table I. Switching states for five-phase seven-level CHBMLI.

Voltage level	HB1				HB2				HB3			
	SW_1	SW_2	SW_3	SW_4	SW_1	SW_2	SW_3	SW_4	SW_1	SW_2	SW_3	SW_4
$+1V_{dc}$	/	×	×	/	×	×	/	/	×	×	/	/
$+2V_{dc}$	/	×	×	/	×	×	/	/	×	×	/	/
$+3V_{dc}$	/	×	×	/	/	×	×	/	/	×	×	/
$0V_{dc}$	×	×	/	/	×	×	/	/	×	×	/	/
$-1V_{dc}$	×	/	/	×	×	×	/	/	×	×	/	/
$-2V_{dc}$	×	/	/	×	×	/	/	×	×	×	/	/
$-3V_{dc}$	×	/	/	×	×	/	/	×	×	/	/	×

Note: '×' indicates off-state; '/' indicates on-state

Table I presents the switching states of the five-phase seven-level CHBMLI required to synthesize the sinusoidal-like staircase output V_{ph} waveform. For each switching state, six switches are turned ON, while the remaining six switches are turned OFF. For instance, to generate a voltage level of $+1V_{dc}$, the following switches are turned ON: HB1-SW_1, HB1-SW_4, HB2-SW_3, HB2-SW_4, HB3-SW_3, and HB3-SW_4. Correspondingly, the switches HB1-SW_2, HB1-SW_3, HB2-SW_1, HB2-SW_2, HB3-SW_1, and HB3-SW_2 are turned OFF. It is important to note that, within each HB module, switches SW_1 and SW_3 or switches SW_2

and SW_4 must never be turned ON simultaneously, as this could cause a shoot-through fault.

III. SELECTIVE HARMONIC ELIMINATION PWM TECHNIQUE

As mentioned earlier, determining the switching angles using SHEPWM technique requires solving a set of multiple harmonic equations. Conventionally, these equations are mathematically derived from the output V_{ph} waveform shown in Fig. 2. Since the waveform is an odd quarter-wave symmetrical waveform, the Fourier series of the V_{ph} is represented as:

$$V_{ph}(\omega t)=\sum_{n=1}^{\infty}\frac{4V_{dc}}{n\pi}\begin{bmatrix}\cos(n\alpha_1)\\+\cos(n\alpha_2)\\+\cos(n\alpha_3)\end{bmatrix}\sin(n\omega t) \quad (1)$$

, where n denotes the n-th harmonic, which is always odd, while ω is the angular frequency. The α_1, α_2, and α_3 must fulfill the conditions as follows:

$$0\le\alpha_1\le\alpha_2\le\alpha_3\le 0.5\pi \quad (2)$$

From Eq. (1), the n-th harmonic of the output phase voltage is presented as:

$$V_n=\frac{4V_{dc}}{n\pi}\begin{bmatrix}\cos(n\alpha_1)+\cos(n\alpha_2)\\+\cos(n\alpha_3)\end{bmatrix} \quad (3)$$

When applying the SHEPWM technique to a five-phase MLI, the fundamental harmonic (V_1) is maintained at a desired value, while the non-quintuple odd harmonics such as V_3, V_7, V_9, V_{11}… are selected to be eliminated. Note that the quintuple odd harmonics, such as V_5, V_{15}, and so on, do not need to be selected for elimination, as they naturally eliminated in the five-phase line-to-line voltage. In a five-phase system, non-quintuple lower order harmonics, e.g., V_3 and V_7, are usually dominant and significantly affect the quality of the inverter output voltage waveform. If these harmonics are not selected to be eliminated, the quality of the output voltage waveform can be poor. Applying such distorted voltage waveform to a motor can cause increased power losses, and in turn reduce the efficiency of five-phase induction machines. Hence, eliminating these harmonics in the five-phase MLI before providing the output voltage for the load is highly desirable. In this case, V_1, V_3, and V_7 are utilized in the SHEPWM technique for the five-phase seven-level CHBMLI. From Eq. (3), the multiple harmonic equations can be presented as below:

$$\begin{aligned}V_1&=\frac{4V_{dc}}{\pi}\left[\cos(\alpha_1)+\cos(\alpha_2)+\cos(\alpha_3)\right]\\V_3&=\frac{4V_{dc}}{3\pi}\left[\cos(3\alpha_1)+\cos(3\alpha_2)+\cos(3\alpha_3)\right]\\V_7&=\frac{4V_{dc}}{7\pi}\left[\cos(7\alpha_1)+\cos(7\alpha_2)+\cos(7\alpha_3)\right]\end{aligned} \quad (4)$$

For a wide range of V_1 control, the V_1 can be modified as:

$$V_1=M\left(\frac{12V_{dc}}{\pi}\right) \quad (5)$$

, where M denotes modulation index ranged from 0 to 1. The main challenge of the SHEPWM technique is solving Eq. (4) to determine the switching angles for the five-phase seven-level CHBMLI. As mentioned earlier, these harmonic equations can be converted into an objective function (OF) and is then solved using SC methods. The OF is presented as follows:

$$\begin{aligned}OF=&\left(100\times\frac{\begin{pmatrix}3M-\cos(\alpha_1)-\\\cos(\alpha_2)-\cos(\alpha_3)\end{pmatrix}}{M}\right)^4\\&+\frac{1}{3}\left(\frac{50\times V_3}{V_1}\right)^2+\frac{1}{7}\left(\frac{50\times V_7}{V_1}\right)^2\end{aligned} \quad (6)$$

Note that the first term of Eq. (6) is used to maintain the V_1 while the second and the third terms are utilized to minimize V_3 and V_7. By minimizing the OF through the SC method, the non-linear transcendental equation derived from Eq. (4) are indirectly solved, and the switching angles for the five-phase seven-level CHBMLI are determined. In this work, the MSA is proposed to solve the SHEPWM problem through minimizing the OF.

IV. MANTIS SEARCH ALGORITHM

The MSA is a nature-inspired swarm-based optimization algorithm that mimics the natural behaviour of praying mantises. This behaviour is modelled in three stages: prey searching, prey attacking, and sexual cannibalism.

A. Prey Searching

In the prey searching stage, mantises aim to explore and perform a global search for the optimal position in the search space. They are divided into two groups: pursuers and spearers. The movement of the pursuer mantises is modelled as follows:

$$y_j^{iter+1} = \begin{cases} y_j^{iter} + \lambda_1 \circ \left(y_j^{iter} - y_a^{iter} \right) \\ + \left| \lambda_2 \right| \cdot W \circ \left(y_a^{iter} - y_b^{iter} \right) & rn_1 \le rn_2 \\ y_j^{iter} \circ W \\ + \left(y_a^{iter} + rv_1 \circ \left(y_b^{iter} - y_c^{iter} \right) \right) \circ \left(1 - W \right) & else \end{cases} \quad (7)$$

, where "○" represents the element-wise product operator and *iter* represents the iteration number. y_j^{iter+1} and y_j^{iter} are the positions of the *j*-th mantis at (*iter*+1)-th and *iter*-th iterations, respectively. In other words, the *j*-th mantis updates its position from y_j^{iter} to y_j^{iter+1}. λ_1 is a vector involving numerical values computed using the Levy flight algorithm, while $|\lambda_2|$ represents a random numerical value generated from a normal distribution, with the mean = 0 and σ = 1. Three mantises are randomly chosen from the mantis swarm and their positions represent y_a^{iter}, y_b^{iter} and y_c^{iter} respectively at current *iter*. rn_1 and rn_2 are the random numerical values ranging from 0 to 1, while rv_1 represents a vector involving random numerical values ranging from 0 to 1. *W* is a binary vector, as shown below:

$$W = \begin{cases} 0 & rv_2 < rv_3 \\ 1 & else \end{cases} \quad (8)$$

, where rv_2 and rv_3 are vectors involving random numerical values. Note that the random numerical values in rn_1, rn_2, rv_1, rv_2, and rv_3 are uniformly distributed. The movement of the spearer mantises is modelled as follows:

$$y_j^{iter+1} = \begin{cases} y_j^{iter} \\ + \Psi \left(\cos \left(\pi rn_3 \right) \right) \left(y_{ar} - y_a^{iter} \right) & rn_5 \le rn_6 \\ y_{ar} \\ + \Psi \circ \left(rn_4 \circ 2 - 1 \right) \circ \left(lb + rv_4 \circ \left(ub - lb \right) \right) & else \end{cases} \quad (9)$$

, where y_{ar} is a mantis chosen randomly from an archive involving the personal best position of each mantis. When the size of the archive reaches its limit, a mantis is randomly selected and replaced with a mantis which has better *OF*. Ψ represents (1 – (*iter* / *maxiter*)) where *maxiter* is the maximum iteration number involved in the MSA, and *lb* and *ub* are the lower and upper boundaries of the search space, respectively. rn_3, rn_4, rn_5, and rn_6 are random numerical values, while rv_4 represents a vector involving random numerical values. Note that these values are uniformly distributed values ranging from 0 to 1. A recycling factor is utilized to categorize the behaviour of mantises into pursuer and spearer types. This factor, denoted as *RF*, is defined as follows:

$$RF = 1 - \left(rmd \left(iter, \left(maxiter / Q \right) \right) / \left(maxiter / Q \right) \right) \quad (10)$$

, where *rmd* is a remainder operator, and *Q* is a constant value used in the initialization of MSA for the trade-off between pursuers and spearers mantises.

B. Prey Attacking

During the prey-attacking stage, mantises focus on exploitation by implementing a local search to refine the solution. The mantises exhibit three types of movement, which are modelled as follows:

$$y_{j,k}^{iter+1} = y_{j,k}^{iter} + rn_7 \cdot \left(y_{a,k}^{iter} - y_{b,k}^{iter} \right) \quad (11)$$

$$y_{j,k}^{iter+1} = \frac{\left(y_{j,k}^{iter} + y^{best} \right)}{2} + \left(\frac{1}{1 + e^{\varepsilon \gamma}} \right) \cdot \left(y^{best} - y_{j,k}^{iter} \right) \quad (12)$$

$$y_{j,k}^{iter+1} = y_{j,k}^{iter} + e^{2\varepsilon} \cdot \cos \left(2\varepsilon \pi \right) \cdot \left| y_{j,k}^{iter} - y_{ar,k} \right| + \left(rn_8 \cdot 2 - 1 \right) \cdot \left(ub - lb \right) \quad (13)$$

, where $y_{j,k}^{iter+1}$ and $y_{j,k}^{iter}$ represent the position of *j*-th mantis in the *k*-th dimension at (*iter*+1)-th and *iter*-th iterations, respectively. In (11), two mantises are randomly chosen from the mantis swarm and their positions denote $y_{a,k}^{iter}$ and $y_{b,k}^{iter}$. In Eq. (12), ε is a numerical value generated randomly within –1 and –2, while γ is the gravitational acceleration rate of the mantis's strike used in the initialization of MSA. y^{best} represents the mantis with the best position (which has the lowest value of *OF*) in the *j*-th dimension. In Eq. (13), a mantis is chosen randomly from the archive and its position denotes $y_{ar,k}$. In these equations, note that rn_7 and rn_8 are uniformly-distributed random numerical values ranging from 0 to 1. During prey-attacking stage, Eq. (13) is utilized with a failure probability (*FP*), where $FP = \beta \cdot \Psi$. Note that β represents a constant value ranging from 0 to 1, which is the striking failure probability. This value is declared in the initialization of MSA.

C. Sexual Cannibalism

Sexual cannibalism is the last stage where the mantises aim to enhance both their exploration and exploitation stage. Three mathematical models are used to represent this stage, as presented below:

$$y_j^{iter+1} = y_j^{iter} \circ W + \left(y_{1,1}^{iter} + rv_5 \circ \left(-y_{1,1}^{iter} + y_j^{iter} \right) \right) \circ \left(1 - W \right) \quad (14)$$

$$y_j^{iter+1} = y_j^{iter} + rv_6 \circ \left(y_j^{iter} - y_a^{iter} \right) \quad (15)$$

$$y_j^{iter+1} = y_a^{iter} \cdot \cos \left(2\pi \varepsilon \right) \cdot \Psi \quad (16)$$

, where $y_{1,1}^{iter}$ denotes the position of the 1-st mantis in the 1-st dimension at *iter*-th iteration. rv_5 and rv_6 are vectors with uniformly-distributed random numerical values ranging from 0 to 1. During the sexual cannibalism stage, mate attraction probability (*MAP*) is utilized with Eq. (15) and Eq. (16), where *MAP* =

$rn_9 \cdot \Psi$. Note that rn_9 is a uniformly-distributed random numerical value ranging from 0 to 1. The overall process of finding the best position using MSA is presented as pseudo code in Fig. 3. Firstly, the parameters such as population size (*PS*), *maxiter*, maximum number of dimensions (*mnd*), length of archive (*LA*), β, exchange probability between mantises in the prey searching and attacking stages (*EP*), γ, Q, and the sexual cannibalism percentage (*SCP*). When applying the MSA to the SHEPWM technique, all the mantises aim to find the position (switching angles) with the minimum *OF* in a search space. In the searching process, the mantises update their positions iteratively using Eqs. (7), (9), (11) to Eq. (13) and Eq. (14) to Eq. (16). The best position of mantis at the last iteration is considered as the switching angles that solve the equations involved in the SHEPWM technique.

Algorithm Pseudo code of MSA

Inputs *PS*, *maxiter*, *mnd*, *LA*, β, *EP*, γ, Q and *SCP*
Initialize the positions of mantises.
Evaluate their *OF* and select the mantis with the min. *OF*.
while (*iter* < *maxiter*)
  Choose a random value (r_1) between 0 and 1
  for *j* = 1: *PS*
    if $r_1 < EP$
      Choose a random value (r_2) between 0 and 1
      Update *RF* using (10)
        if $r_2 < RF$
          Update y_j^{iter+1} using (7)
        else
          Update y_j^{iter+1} using (9)
        end if
        Calculate *OF* of mantis with position y_j^{iter+1},
        Replace y_j^{iter} with y_j^{iter+1} if y_j^{iter+1} has better *OF*
    else
      Choose a random value (r_3) between 0 and 1
      for *k* = 1: *mnd*
      Choose a random value (r_4) between 0 and 1
        if $r_4 < r_3$
          Update $y_{j,k}^{iter}$ using (11)
        else
          Update $y_{j,k}^{iter}$ using (12)
          if $r_3 < FP$
            Update $y_{j,k}^{iter}$ using (13)
          end if
        end if
      end for
      Calculate *OF* of mantis with position y_j^{iter+1}
      Replace y_j^{iter} with y_j^{iter+1} if y_j^{iter+1} has better *OF*
      Update *FP*
    end if
  end for
  if $r_1 < EP$
    for *j* = 1: *PS*
      Choose a random value (r_5) between 0 and 1
      Choose a random value (r_6) between 0 and 1
      if $r_5 < r_6$
        Update y_i^{iter} using (14)
      else
        if $r_6 < MAP$
          Update y_j^{iter} using (15)
        else
          Update y_j^{iter} using (16)
        end if
      end if
      Calculate *OF* of mantis with position y_j^{iter+1}
      Replace y_j^{iter} with y_j^{iter+1} if y_j^{iter+1} has better *OF*
      Updating *MAP*
    end for
  end if
  update y^{best} if there is a better solution
  iter = *iter* + 1
end while
Outputs y^{best} is selected as the final solution

Fig. 3. Pseudo code of MSA.

V. RESULTS AND DISCUSSION

In this work, MATLAB analysis is used to evaluate the performance of MSA in solving SHEPWM problem for five-phase seven-level CHBMLI. The performance of MSA is validated by comparing it with popular SC methods: GA and PSO. For a fair comparison, all SC methods are initialized with the same parameters: a *PS* of 100 and a *maxiter* of 500. Each SC method is executed 20 times to increase the probability of obtaining better switching angles. These SC methods aim to minimize the *OF* defined in Eq. (6), over a wide *M* range, where *M* = 0.01:0.01:1.00. Figure 4 presents a comparison of the resulting *OF* values. As shown in the figure, at *M* = 0.46, *M* = 0.57 to *M* = 0.66, and *M* = 0.76 to *M* = 0.85, the *OF* values provided by MSA are between 10^{-25} and 10^{-33}, which are significantly lower than those obtained by GA and PSO. According to Eq. (6), minimizing the *OF* reduces its first term—the difference between V_1 and the desired fundamental harmonic, which indicating improved accuracy in achieving the desired fundamental harmonic. At the same time, the second and third terms, which represent undesired low order harmonics (V_3 and V_7), are also minimized. Therefore, if an SC method achieves a lower *OF*, it implies that the SC method has found better switching angles. As shown in Fig. 4, the *OF* values of the MSA are lower than those of the GA and PSO, indicating the switching angles of the MSA are better than both methods. Figure 5 presents the cumulative distribution function (*CDF*) of the *OF* results obtained by GA, PSO, and MSA. The *CDF* is expressed as follows:

$$CDF = Percent\left(OF \le OF_{\mathrm{d}}\right) \tag{17}$$

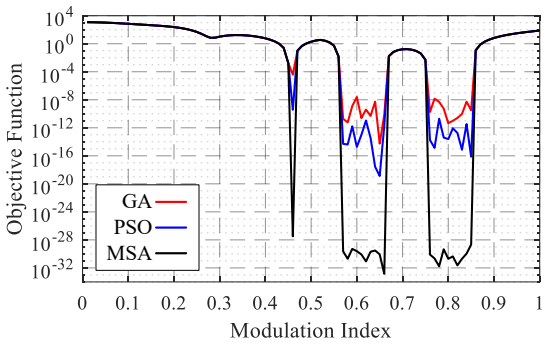

Fig. 4. *OF*s achieved by MSA, GA and PSO.

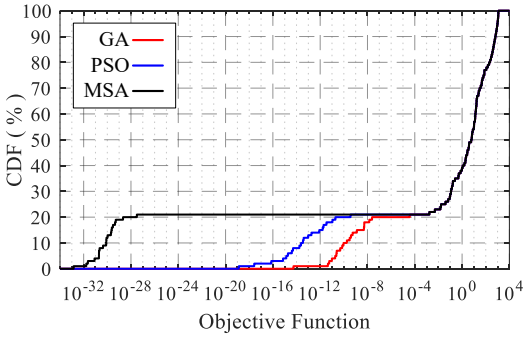

Fig. 5. *CDF*s achieved by MSA, GA and PSO.

The *CDF* represents the probability or the percentage (*Percent*) of an *OF* value equal to or lower than a defined *OF* (OF_{d}) value. As shown in Fig. 5, at

OF value of 10^{-25}, the *CDF* of MSA is 21 %, while the *CDF*s of GA and PSO remain at 0 %. This result indicates that the proposed MSA has a higher probability of achieving lower *OF* values compared to GA and PSO. MSA employs several alternative search strategies, such as prey searching, prey attacking and sexual cannibalism, for finding better solution, which offer better exploration and exploitation compared to GA and PSO. As a result, these strategies enable MSA to achieve a higher chance of finding better solutions, thereby achieving lower OF values. Figure 6 shows the switching angles provided by MSA for solving SHEPWM problem of five-phase seven-level CHBMLI. The figure shows that the MSA-SHEPWM technique is capable of generating switching angles over a wide *M* range while satisfying the condition given in Eq. (2).

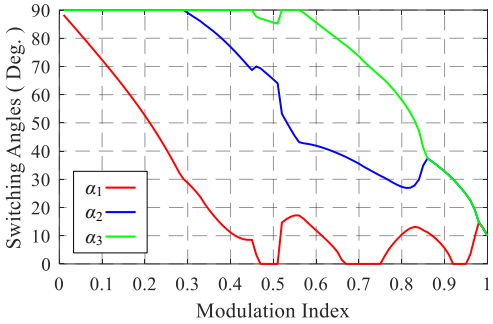

Fig. 6. Switching angles provided by MSA for solving SHEPWM problem of five-phase seven-level CHBMLI.

The effectiveness of the switching angles provided by MSA is validated through harmonic response analysis (harmonic calculation using Eq. (4)), as illustrated in Fig. 7. The figure shows that MSA is capable of maintaining the desired fundamental harmonic (V_1) at nearly 100 % over a wide *M* range, at the same time minimizing undesired low order harmonics (V_3 and V_7). As can be seen in the figure, at $M = 0.46$, $M = 0.57$ to $M = 0.66$, and $M = 0.76$ to $M = 0.85$, the values of V_3 and V_7 are very close to zero, indicating successful harmonic minimization. This outcome is mainly contributed by the successful *OF* minimization achieved by MSA shown in Fig. 4. Therefore, the results from Figs. 6 and 7 validate that the switching angles obtained using MSA enable the five-phase seven-level CHBMLI to produce an output voltage in which V_1 is maintained close to the desired value, and at the same time the undesired harmonics are minimized.

For further validation, a set of switching angles is selected from Fig. 6 and applied to a PSIM simulation model of a five-phase seven-level CHBMLI to generate V_{ph} and line-to-line voltage (V_{line}) waveforms. The following simulation results are generated using the switching-angle set at $M = 0.85$, where $\alpha_1 = 11.96°$, $\alpha_2 = 34.89°$, and $\alpha_3 = 41.28°$. The switching angles applied to phases B, C, D and E of the CHBMLI are phase-shifted by 72°, 144°, 216° and 288°, respectively, from phase A due to the five-phase configuration of the CHBMLI. In the CHBMLI, the magnitude of each DC voltage source is set to 10 V, and the load is 30 Ω. Note that each switch in the CHBMLI is operated at fundamental frequency of 50 Hz. In the PSIM simulation, the magnitude of the first ten odd harmonics in the V_{ph} and V_{line} waveforms are given using the Fast Fourier Transform (FFT).

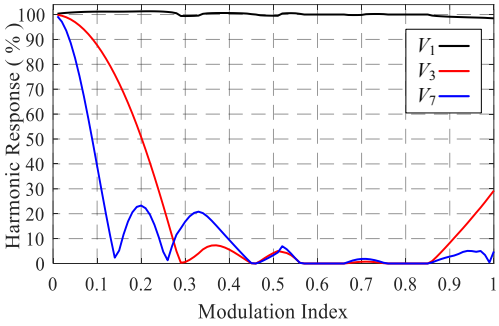

Fig. 7. Harmonic response achieved by the switching angles provided by MSA for five-phase seven-level CHBMLI.

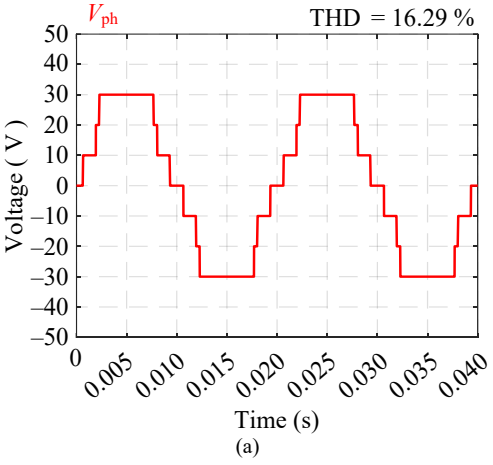

(a)

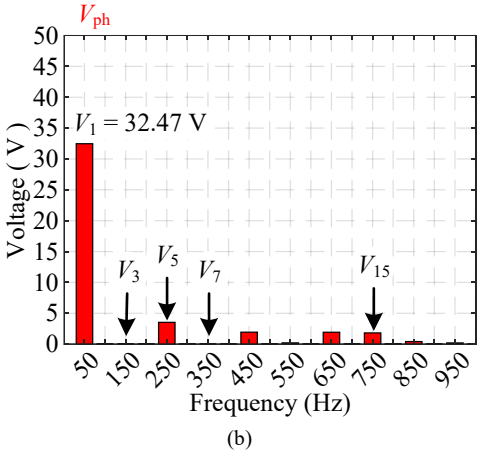

(b)

Fig. 8. V_{ph} generated by the five-phase seven-level CHBMLI at $M = 0.85$ using MSA switching angles. (a) Waveform (b) FFT plot.

Figures 8(a) and 8(b) present the output V_{ph} waveform and its corresponding FFT analysis, respectively, for the five-phase seven-level CHBMLI operating at $M = 0.85$, using the switching angles given by MSA. As can be seen in Fig. 8(a), the voltage waveform is likely sinusoidal, with a THD of 16.29 %.

As shown in Fig. 8(b), the magnitude of the V_1 is 32.47 V, which matches the desired value calculated using Eq. (5). In addition, the magnitude of V_3 and V_7 are zero. Hence, these results further confirm that the switching angles obtained using the MSA can maintain the desired V_1 while minimizing undesired low order harmonics. Figures 9(a) and 9(b) present the output V_{line} waveform and its FFT analysis for the five-phase seven-level CHBMLI using the same switching angles given by MSA. As shown in Fig. 9(a), the V_{line} waveform has a higher number of voltage levels compared to the V_{ph} waveform shown in Fig. 8(a). Since a staircase voltage waveform with higher number of voltage levels has higher chance to achieve lower THD, the V_{line} THD shown in Fig. 9(a) is lower than V_{ph} THD shown in Fig. 8(a). As shown in Fig. 9(b), the V_3 and V_7 in line-to-line voltage are zero. In addition, the quintuple odd harmonics such as V_5 and V_{15} are also zero. As mentioned earlier, the quintuple odd harmonics are eliminated due to the five-phase configuration of the MLI. As a result, the V_{line} THD will be lower than V_{ph} THD since more harmonics are eliminated in V_{line} compared to V_{ph}. Hence, the results from Figs. 8 and 9 validate that MSA switching angles enable the MLI to produce an AC output voltage with reduced THD.

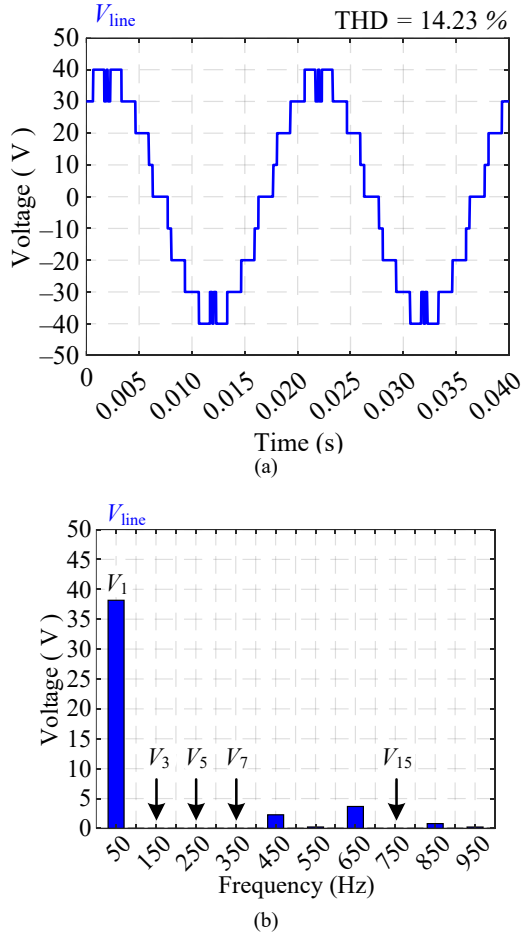

Fig. 9. V_{line} generated by the five-phase seven-level CHBMLI at M = 0.85 using MSA switching angles. (a) Waveform (b) FFT plot.

VI. CONCLUSION

This paper presents the performance of the MSA in solving the SHEPWM problem for determining switching angles of a five-phase MLI. MATLAB analysis results demonstrate that MSA achieves better *OF* minimization compared to GA and PSO. By minimizing the *OF*, MSA can generate switching angles over a wide M range. The switching angles can minimize selected undesired low-order harmonics (V_3 and V_7) while maintaining the desired fundamental harmonic (V_1). PSIM simulation results further validate that, when the switching angles obtained by MSA are applied to a five-phase seven-level CHBMLI, the inverter produces staircase output voltage waveforms with reduced THD. In these waveforms, the desired fundamental voltage is satisfied, and the selected low-order harmonics are minimized. These findings align with the MATLAB-based analysis, confirming that MSA can be applied in the SHEPWM technique to produce low-distorted AC output voltage waveforms for five-phase MLIs.

ACKNOWLEDGEMENT

This work was supported by the Ministry of Higher Education Malaysia through the Fundamental Research Grant Scheme (FRGS/1/2020/TK0/UNIMAP/02/54).

FUNDING STATEMENT

The authors received no funding from any party for the research and publication of this article.

AUTHOR CONTRIBUTIONS

Quan Ming Wong: Writing, Original Draft Preparation, Reviewing and Editing;
Wei Tik Chew: Resources, Formal Analysis, Investigation;
Yee Wei Sea: Methodology, Validation, Visualization;
Siok Lan Ong: Paper Reviewing, Supervision;
Noor Syafawati Ahmad: Paper Reviewing and Supervision;
Ahmad Firdaus Ahmad Zaidi: Paper Reviewing and Supervision;
Jenn Hwai Leong: Paper Reviewing and Supervision.

CONFLICT OF INTERESTS

No conflict of interests was disclosed.

ETHICS STATEMENTS

Our publication ethics follow The Committee of Publication Ethics (COPE) guideline. https://publicationethics.org/

REFERENCES

[1] P. Albrechtowicz, "Electric Vehicle Impact on The Environment in Terms of The Electric Energy Source — Case Study," *Ener. Rep.*, vol. 9, pp. 3813–3821, 2023.
[2] N. A. Q. Muzir, M. R. H. Mojumder, M. Hasanuzzaman and J. Selvaraj, "Challenges of Electric Vehicles and Their Prospects in Malaysia: A Comprehensive Review," *Sustainability*, vol. 14, no. 14, pp. 8320, 2022.
[3] J. Kellner, S. Kaščák and Ž. Ferková, "Investigation of The Properties of A Five-Phase Induction Motor in the Introduction

of New Fault-Tolerant Control," *Appl. Sci.,* vol. 12, no. 4, pp. 2249, 2022.

[4] A. Poorfakhraei, M. Narimani and A. Emadi, "A Review of Multilevel Inverter Topologies in Electric Vehicles: Current Status and Future Trends," *IEEE Open J. Pow. Electron.*, vol. 2, pp. 155–170, 2021.

[5] A. Iqbal, A. Awadelseed and J. Guzinski, "High-Efficiency Switched-Capacitor Multilevel Inverter Topology with Lower Number of Switching Components," *IEEE Access*, vol. 13, pp. 84941–84953, 2025.

[6] N. Karania, M. A. Alali, S. D. Gennaro and J. Barbot, "Advanced High Switching-Frequency Cascaded H-Bridge Multilevel Inverter-Based Shunt Active Filter for PV Generation: A Case Study," *IEEE Open J. Indust. Appl.*, vol. 6, pp. 262–280, 2025.

[7] E. Babaei, S. Laali and S. Alilu, "Cascaded Multilevel Inverter with Series Connection of Novel H-Bridge Basic Units," *IEEE Trans. Indust. Electron.*, vol. 61, no. 12, pp. 6664–6671, 2014.

[8] Ó. López *et al*., "Postfault Operation Strategy for Cascaded H-Bridge Inverters Driving A Multiphase Motor," *IEEE Trans. Indust. Electron.*, vol. 71, no. 5, pp. 4309–4319, 2024.

[9] Z. Pan and F. Z. Peng, "A Sinusoidal PWM Method With Voltage Balancing Capability for Diode-Clamped Five-Level Converters," *IEEE Trans. Indust. Appl.*, vol. 45, no. 3, pp. 1028–1034, 2009.

[10] M. A. Al-Hitmi, S. Moinoddin, A. Iqbal, K. Rahman and M. Meraj, "Space Vector vs. Sinusoidal Carrier-Based Pulse Width Modulation for a Seven-Phase Voltage Source Inverter," *CPSS Trans. Pow. Electron. and Appl.*, vol. 4, no. 3, pp. 230–243, 2019.

[11] D. Zhou, S. Liu, J. Tan, J. Zou and X. Liu, "Dual-Layer SVM-Based Power Flow Control of ANPC-Type Multiport Inverter in Multisource Electric Vehicles," *IEEE Trans. Pow. Electron.*, vol. 40, no. 12, pp. 18448-18460, 2025.

[12] A. R. Ansari, A. Shahzad Siddiqui, A. Sarwar, M. Khursheed and D. D. Sharma, "Comparison Analysis of Performance of Different PWM Techniques Used in Multilevel Inverters," in *Proc. 2024 2nd Int. Conf. Computat. and Characteriz. Techn. in Eng. & Sci.*, Lucknow, India, pp. 1–7, 2024.

[13] P. Kalkal and A. V. R. Teja, "Selective Harmonic Elimination PWM Technique Based on Higher Order Sliding Modes: Generalized Formulation," *IEEE J. Emer. and Select. Topics in Pow. Electron.*, vol. 12, no. 1, pp. 631–640, 2024.

[14] L. Manai, M. Dabboussi, F. Armi and M. Besbes, "Cascaded Multilevel Inverter Control Considering Low Harmonic Content Based on Comparison Study Between Firefly and Newton Raphson Algorithm," in *Proc. 2016 4th Int. Conf. Contr. Eng. & Inform. Technol.*, Hammamet, Tunisia, pp. 1–5, 2016.

[15] A. R. Lopez *et al*., "Harmonic Mitigation in A Multilevel Inverter with The Newton Raphson Method and The Particle Swarm Optimization," in *Proc. 2021 IEEE Int. Autumn Meeting on Pow., Electron. and Comput.*, Ixtapa, Mexico, pp. 1–6, 2021.

[16] J. N. Chiasson, L. M. Tolbert, K. J. McKenzie and Z. Du, "Control of a Multilevel Converter Using Resultant Theory," *IEEE Trans. Contr. Syst. Technol.*, vol. 11, no. 3, pp. 345–354, 2003.

[17] J. N. Chiasson, L. M. Tolbert, K. J. McKenzie and Z. Du, "Elimination of Harmonics in A Multilevel Converter Using The Theory of Symmetric Polynomials and Resultants," *IEEE Trans. Contr. Syst. Technol.*, vol. 13, no. 2, pp. 216–223, 2005.

[18] D. G. Kumar, N. V. Sireesha, N. Bhoopal, R. K. Gatla, H. Kotb, K. M. AboRas, A. Elrashidi, M. Alqarni, Y. Y. Ghadi and A. Oubelaid, "Application of Soft Computing Algorithms for Hybrid Modular Multilevel Inverters," *Measurement: Sensors*, vol. 31, pp. 100999, 2024.

[19] C. Sámano *et al*., "FPGA Implementation of Genetic Algorithm-Driven Commutation for H-Bridge Inverters," in *Proc. 2024 IEEE Int. Autumn Meeting on Pow., Electron. and Comput.*, Ixtapa, Mexico, pp. 1–6, 2024.

[20] A. Ghasemian, S. Mohamadian, C. Buccella, M. G. Cimoroni and C. Cecati, "Selective Harmonic Mitigation of Cascaded H-Bridge Multilevel Converters Using Real-Coded Genetic Algorithm," in *Proc. 2024 IEEE Int. Conf. on Artif. Intellig. & Green Ener.*, Yasmine Hammamet, Tunisia, pp. 1–6, 2024.

[21] R. Tota, L. Tasnim, S. M. Akash and M. Rahman, "Evolutionary Algorithm-Based Approach to Reduce Total Harmonic Distortion for Symmetrical 7-Level Inverter," in *Proc. 2024 IEEE Int. Conf. on Pow., Electr., Electron. and Industr. Appl.*, Rajshahi, Bangladesh, pp. 557–562, 2024.

[22] M. Abdel-Basset, R. Mohamed, M. Zidan, M. Jameel and M. Abouhawwash, "Mantis Search Algorithm: A Novel Bio-Inspired Algorithm for Global Optimization and Engineering Design Problems," *Comput. Methods Appl. Mech. Eng.*, vol. 415, pp. 116200, 2023.

[23] L. Gowrisankar, J. G. Murali and Y. D. Ravichandiran, "Characterization of Integrated Nanomaterials Using Deep Learning Method-Based Mantis Search Algorithm," *J. Comput. Electron.*, vol. 24, no. 2, pp. 46, 2025.

[24] G. Moustafa *et al.*, "An Advanced Bio-Inspired Mantis Search Algorithm for Characterization of PV Panel and Global Optimization of Its Model Parameters," *Biomimetics*, vol. 8, no. 6, pp. 490, 2023.

[25] G. Moustafa *et al*., "A Novel Mantis Search Algorithm for Economic Dispatch in Combined Heat and Power Systems," *IEEE Access*, vol. 12, pp. 2674–2689, 2024.

[26] R. Gowravaram, "Adaptive Parameter-Based Mantis Search Algorithm and Regularized Dropout with Gated Recurrent Unit for Multimodal Biometric Recognition," *Int. J. Intell. Eng. Syst.*, vol. 18, pp. 521–532, 2025.

[27] Z. Fei, Y. Li and S. Yang, "Pattern Recognition of Partial Discharge Faults in Switchgear Using A Back Propagation Neural Network Optimized by An Improved Mantis Search Algorithm," *Sensors*, vol. 24, no. 10, pp. 3174, 2024.